



# GIP1 and GIP2 Contribute to the Maintenance of Genome Stability at the Nuclear Periphery

Gaurav Singh<sup>1</sup>, Morgane Batzenschlager<sup>2</sup>, Denisa Tomkova<sup>1</sup>, Etienne Herzog<sup>1</sup>, Elise Hoffmann<sup>1</sup>, Guy Houlné<sup>1</sup>, Anne-Catherine Schmit<sup>1</sup>, Alexandre Berr<sup>1</sup> and Marie-Edith Chabouté<sup>1\*</sup>

<sup>1</sup> Institut de Biologie Moléculaire des Plantes, CNRS, Université de Strasbourg, Strasbourg, France, <sup>2</sup> Cell Biology, Faculty of Biology, University of Freiburg, Freiburg, Germany

## OPEN ACCESS

### Edited by:

Yangnan Gu,  
University of California, Berkeley,  
United States

### Reviewed by:

Chang Liu,  
University of Hohenheim, Germany  
Yu Tang,  
University of California, Berkeley,  
United States

### \*Correspondence:

Marie-Edith Chabouté  
marie-edith.chaboute@  
ibmp-cnrs.unistra.fr

### Specialty section:

This article was submitted to  
Plant Cell Biology,  
a section of the journal  
Frontiers in Plant Science

**Received:** 29 October 2021

**Accepted:** 20 December 2021

**Published:** 27 January 2022

### Citation:

Singh G, Batzenschlager M, Tomkova D, Herzog E, Hoffmann E, Houlné G, Schmit A-C, Berr A and Chabouté M-E (2022) GIP1 and GIP2 Contribute to the Maintenance of Genome Stability at the Nuclear Periphery. *Front. Plant Sci.* 12:804928. doi: 10.3389/fpls.2021.804928

The maintenance of genetic information is important in eukaryotes notably through mechanisms occurring at the nuclear periphery where inner nuclear membrane proteins and nuclear pore-associated components are key factors regulating the DNA damage response (DDR). However, this aspect of DDR regulation is still poorly documented in plants. We addressed here how genomic stability is impaired in the *gamma-tubulin complex component 3-interacting protein (gip1gip2)* double mutants showing defective nuclear shaping. Using neutral comet assays for DNA double-strand breaks (DSBs) detection, we showed that GIP1 and GIP2 act redundantly to maintain genome stability. At the cellular level,  $\gamma$ -H2AX foci in *gip1gip2* were more abundant and heterogeneous in their size compared to wild-type (WT) in root meristematic nuclei, indicative of constitutive DNA damage. This was linked to a constitutive activation of the DDR in the *gip1gip2* mutant, with more emphasis on the homologous recombination (HR) repair pathway. In addition, we noticed the presence of numerous RAD51 foci which did not colocalize with  $\gamma$ -H2AX foci. The expression of GIP1-GFP in the double mutant rescued the cellular response to DNA damage, leading to the systematic colocalization of RAD51 and  $\gamma$ -H2AX foci. Interestingly, a significant proportion of RAD51 foci colocalized with GIP1-GFP at the nuclear periphery. Altogether, our data suggest that GIPs may partly contribute to the spatio-temporal recruitment of RAD51 at the nuclear periphery.

**Keywords:** *A. thaliana*, genome stability, root meristem, GIP, RAD51 foci,  $\gamma$ -H2AX foci

## INTRODUCTION

Safeguarding the genetic information is essential in cells under endogenous and exogenous stresses leading to DNA damage. The integrity of genetic information has also to be maintained in cycling cells during DNA replication and during mitosis. In eukaryotes, DNA lesions lead to the activation of specific networks of proteins which are recruited at DNA damage sites for signaling and repair.

Plants are constantly facing environmental stresses leading to various forms of DNA lesions, with DNA double-strand breaks (DSBs) as the most serious form of DNA damage (West et al., 2004). Besides their induction by exogenous genotoxic stresses, DSBs can also arise either from DNA replication defects such as stalling replication fork or as a result of an increased level of

endogenous Reactive Oxygen Species (ROS). Un-repaired or mis-repaired DSBs in dividing cells can lead to the formation of aberrant chromosomes and thus to developmental defects (Roy, 2014). DSBs repair is mainly mediated by either Homologous Recombination (HR) or Non-homologous End Joining (NHEJ) (West et al., 2004). In this context, chromatin organization around damage sites plays also a crucial role in the DNA damage response (DDR) by providing a scaffold and/or easy access to the DNA repair machinery (Takatsuka et al., 2021). The  $\gamma$ -H2AX protein (a phosphorylated form of the histone variant H2AX) accumulates at DSBs (Friesner et al., 2005) and is instrumental for the recruitment of DNA repair signaling and repair factors (Lang et al., 2012; Amiard et al., 2013; Biedermann et al., 2017; Horvath et al., 2017). Besides the recruitment at DSBs of BREAST CANCER SUSCEPTIBILITY1 (BRCA1), RADIATION SENSITIVE51 (RAD51), and RAD54 which are involved in HR (Biedermann et al., 2017; Hirakawa et al., 2017; Horvath et al., 2017), the RETINOBLASTOMA-RELATED 1 (RBR1) and the transcription factors E2Fa are also found at DSBs to promote HR (Lang et al., 2012; Biedermann et al., 2017; Horvath et al., 2017; Raynaud and Nisa, 2020). More recently, the important cell-cycle regulatory protein F-BOX-LIKE17 (FBL17) was shown to be a regulator of the DDR and to colocalize as well with RBR1 and  $\gamma$ -H2AX at DNA lesions, suggesting connections between cell cycle and DDR in plants (Gentric et al., 2020, 2021).

In mammals the nucleo-cytoplasmic interface and its associated protein complexes, such as the nuclear pore complex (NPC), the LINC complexes (Linker of Nucleoskeleton and Cytoskeleton) or the nuclear lamina play critical roles in regulating DDR (Bukata et al., 2013; Ryu et al., 2015). However, such regulatory processes, in the context of the nuclear envelope (NE) environment, still remain poorly investigated in plants. The SAD1/UNC-84 (SUN1 and SUN2) domain proteins, belonging to the LINC complexes, at the inner nuclear membrane of the NE regulate meiotic recombination (Varas et al., 2015). RAD54, required for HR in somatic cells, forms foci in response to irradiation in *Arabidopsis* root cell nuclei that accumulate at the nuclear periphery (Hirakawa and Matsunaga, 2019). As components of the plant nucleoskeleton, CROWDED NUCLEI (CRWN) proteins protect genomic DNA against excessive oxidative damages caused by the DNA damaging agent methyl methanesulfonate (Wang et al., 2019). Finally, the HIGH EXPRESSION OF OSMOTICALLY RESPONSIVE GENE1 (HOS1), as part of the NPC (Cheng et al., 2020), was recently reported to activate DNA repair components in response to heat-induced DNA damages (Han et al., 2020).

Previously, we showed that the gamma-tubulin complex component 3-interacting proteins (GIPs), located on both side of the NE, are key players in regulating the plant nuclear architecture and organization, notably through the maintenance of centromeric cohesion at the nuclear periphery of *Arabidopsis* root meristem nuclei (Janski et al., 2012; Batzenschlager et al., 2013; Batzenschlager et al., 2015; Chabouté and Berr, 2016). In this work, using cellular and molecular experimental approaches, we detected numerous endogenous  $\gamma$ -H2AX foci, indicative of constitutive DSBs, as well as the preferential activation of the

HR signaling pathway in *gip1gip2*. This might rely on defective HR repair linked to impaired colocalization of  $\gamma$ -H2AX with the DNA repair protein RAD51 involved in HR. However, upon genotoxic stress this colocalization is restored in the *gip1gip2* mutant complemented by the expression of a GIP1-GFP fusion protein. Finally, we also detected a partial but significant colocalization between GIP1-GFP and RAD51 foci at the nuclear periphery. Together, our findings shed light on the contribution of GIPs at the nuclear periphery for genome maintenance and proper localization of RAD51 foci.

## MATERIALS AND METHODS

### Plants, Growth, and Treatment Conditions

The mutants *gip1*, *gip2*, *gip1gip2* and their corresponding genetic background Col-0, WS, and Col-0 x WS have been described previously (Janski et al., 2012; Batzenschlager et al., 2017). *Arabidopsis* seedlings were grown *in vitro* on  $\frac{1}{2}$  Murashige and Skoog medium (SERVA Electrophoresis) in presence of 1% sucrose supplemented with 1.2% agar at 20°C under long day conditions (16-h light 70  $\mu\text{mol m}^{-2} \text{s}^{-1}$  of fluorescent lighting/8-h dark). The *gip1gip2* mutant was complemented by the expression of a pGIP1::GIP1-GFP construct as previously described (Janski et al., 2012; Batzenschlager et al., 2015). For sensitivity tests to genotoxic drugs, seeds were initially sowed on  $\frac{1}{2}$  MS agar and after 5 days on growth, seedlings were transferred on media supplemented with the genotoxins. Drug concentrations were 10  $\mu\text{M}$  for Bleomycin (BLM) (Laboratoire Thissen, Belgium) and 50  $\mu\text{M}$  for cisplatin (CP) (Sigma, St. Louis, United States). Seedlings were treated during 16 h by 50  $\mu\text{M}$  CP in  $\frac{1}{2}$  MS for cytological analyses.

### Neutral Comet Assay

Nuclei were isolated from 9-day-old seedlings using a Chopping solution and comet assays were performed as described (Roa et al., 2009; Lang et al., 2012). The quantification of the comet figures was related to an arbitrary scoring of the comet figures as described previously (Collins, 2004). In each assay, 100 comets were scored and the results represent the mean values from three independent experiments.

### Immunostaining

Nine-day-old *Arabidopsis* seedlings were fixed in 4% PFA and processed as described previously on nuclei from squashed root tip (Batzenschlager et al., 2015). The primary anti- $\gamma$ -H2AX antibody (diluted at 1/500) produced by Davids Biotechnology (Regensburg, Germany; Friesner et al., 2005), the rat anti-RAD51 antibody (diluted at 1/500) (Kerzendorfer et al., 2006) and when needed the monoclonal antibody directed against GFP (diluted at 1/500) (Invitrogen, Thermo Fisher Scientific) were incubated overnight at 4°C. Signals were revealed accordingly with the following secondary antibodies: Alexa fluor-488 goat anti-rabbit (diluted at 1/200), the Alexa fluor-488 goat anti-mouse (diluted at 1/200), the Alexa fluor-568 goat anti-rat (diluted at 1/300) and

the Cy5 goat anti-rabbit (diluted at 1/300) (Life Technologies, Thermo Fisher Scientific). Root tips were mounted in antifade Vectashield (Vector Laboratories), with DAPI (2  $\mu\text{g}/\text{ml}$ ).

## Confocal Analyses

Confocal images were recorded with a Zeiss LSM 780 microscope equipped with an oil 63  $\times$  /1.4 NA lens. The excitation and emission wavelengths for Alexa 488 were 488 and 510 nm, respectively. To reveal Alexa 568, the excitation and emission wavelengths were 555 and 617 nm, respectively. For DAPI observations, the excitation and emission wavelengths were 405 and 500 nm, respectively. Cy5 was combined with DAPI, with excitation and emission wavelengths of 571 and 735 nm, respectively. Observations were performed in multi-tracking mode using 405-, 488-, or 561-nm laser excitation. Images were processed using the ImageJ software.

## RNA Extraction and Real-Time RT-qPCR

Total RNA was extracted from 9-day-old *Arabidopsis thaliana* seedlings using the Nucleospin RNA Plant kit (Macherey-Nagel, Hoerd, France) according to manufacturer's instructions after grinding with glass beads (1, 7/2 mm) in a Precellys<sup>®</sup>24 grinder (Bertin Technologies, Saint-Quentin-en-Yvelines, France) at 5,500 rpm, 2  $\times$  30 s. For RT-qPCR, 2.5  $\mu\text{g}$  of RNA were used to synthesize cDNA using specific primers, random hexamer primers (IDT) and the protocol "SuperScript<sup>®</sup> IV (SSIV) First-strand and cDNA Synthesis Reaction" (Invitrogen). RT-qPCR was performed on a LightCycler 480 II (Roche) with SYBR Green Master Mix (Bio-Rad), according to the manufacturer's instructions. All primers used are described in **Supplementary Table 1**. Quantification was done using the  $\Delta\Delta\text{Ct}$  method and normalized to ACTIN2 (Livak and Schmittgen, 2001).

## RESULTS

### High Genomic Instability Is Linked to Endogenous Double-Strand Breaks in *gip1gip2*

Our previous data have shown that chromosome instability occurs during mitosis in the *gip1gip2* double mutant, resulting in the appearance of micronuclei in interphase cells and ploidy defects (Janski et al., 2012; Batzenschlager et al., 2015). Because micronuclei may result as well from mis-repaired and/or unrepaired DNA DSBs (Fenech et al., 2011; Ye et al., 2019) we decided to explore whether DSB repair is affected in *gip1gip2*. Firstly, DSBs were detected and quantified using the neutral comet assay. Our analyses were performed on isolated nuclei from *gip1gip2* seedlings showing a strong phenotype (Batzenschlager et al., 2015), the single mutants *gip1* and *gip2* and on nuclei of the corresponding WT controls (i.e., Col-0xWS, WS, and Col-0). Compared to their respective controls, comet tails appeared increased in both single and double *gip* mutants (**Figure 1A**). In order to quantify more precisely their respective genomic instability, DNA damage was evaluated upon visual scoring of each individual comet tail as previously described (Ro

et al., 2009). While *gip1* and *gip2* presented about 1.4 times more DSBs than their respective WT control, *gip1gip2* showed 2.4 times more DSBs than Col-0xWS (**Figure 1B**). Altogether, our data suggest that *GIP1* and *GIP2* may have some overlapping functions to maintain genome stability and to limit DNA damages in interphase nuclei under normal growth conditions.

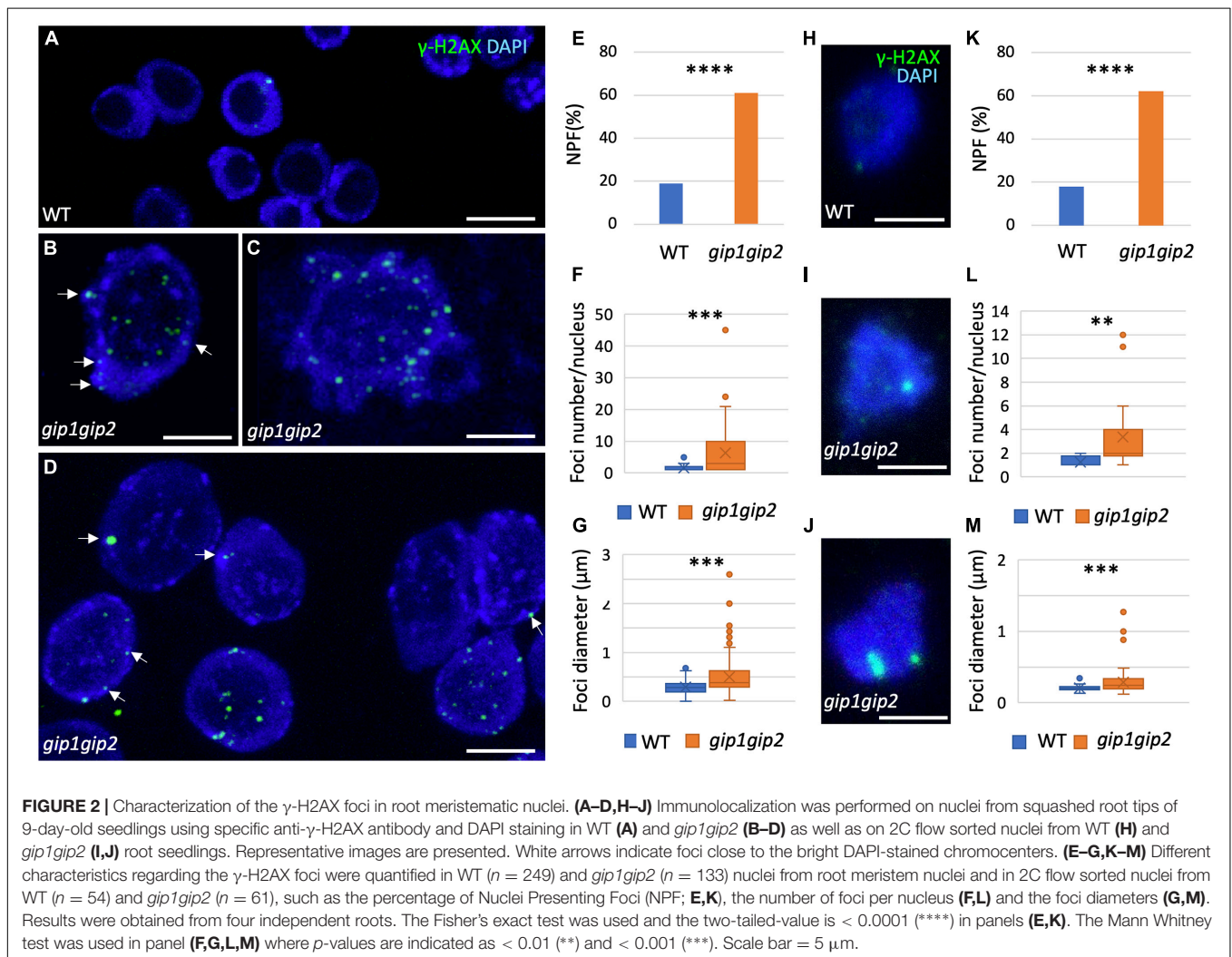
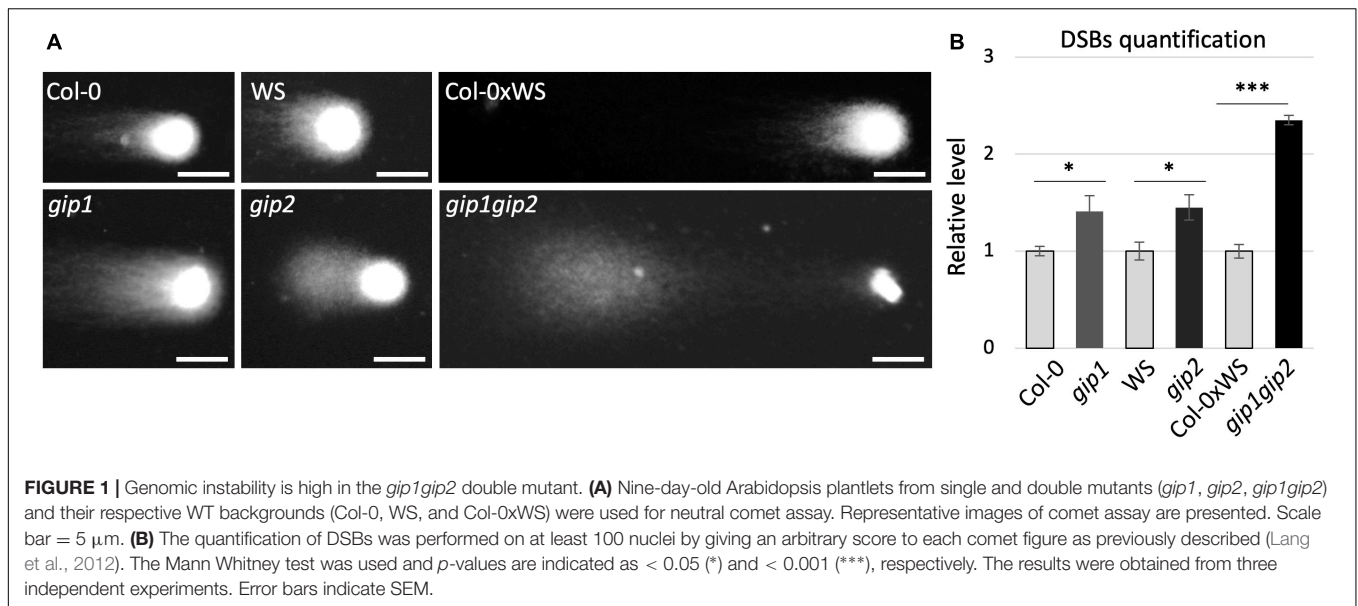
### Nuclear $\gamma$ -H2AX Foci Are Highly Heterogenous in Size and Number in *gip1gip2*

To further analyze the significant increase of DSBs in *gip1gip2* and determine their localization at the cellular level in root meristematic nuclei, we performed immunolocalization with an antibody directed against  $\gamma$ -H2AX, a phosphorylated form of the H2AX histone variant known to be associated with sites of DSBs (Lang et al., 2012). Compared to the low occurrence of nuclei showing  $\gamma$ -H2AX foci in WT, the *gip1gip2* double mutant showed a significantly higher proportion of nuclei with foci and, frequently, several foci per nucleus (**Figures 2A–D**). The foci were found in the nucleoplasm, around the nucleolus and at the nuclear periphery. Among them, 22% were associated to the chromocenters (**Figures 2B–D**, see white arrows).

The  $\gamma$ -H2AX foci were observed in 19% of the nuclei in the WT control (hereafter named NPF for Nuclei Presenting Foci), while the proportion of NPF was 3.2 times higher in the double mutant (**Figure 2E**). Moreover, compared to the WT control in which a mean of 1 focus per nucleus was evaluated, the number of foci per nucleus was significantly increased in the double mutant, reaching a mean of  $6 \pm 1$  foci/nucleus (**Figure 2F**). While the foci mean diameter was relatively homogenous in the WT control with a mean of 0.3  $\mu\text{m}$  ranging from 0.1 to 0.7  $\mu\text{m}$ , it appeared larger in the double mutant with a mean of 0.5  $\mu\text{m}$  and strongly heterogeneous with diameters ranging from 0.2 to 2.5  $\mu\text{m}$  (**Figure 2G**).

Previously, *gip1gip2* plants were described to display ploidy instability (Janski et al., 2012; Batzenschlager et al., 2015). To disentangle appearance of  $\gamma$ -H2AX foci from ploidy defects, we next focused our analysis on 2C flow sorted nuclei from root seedlings (**Figures 2H–M**). Proportions of NPF in the WT control (18%) and the *gip1gip2* double mutant (62%) (**Figure 2K**) were similar as for root meristematic nuclei (**Figure 2E**). In addition, both the number of foci per nucleus and their individual sizes were significantly higher in the double mutant compared to the WT control (**Figures 2L,M**). Indeed, WT nuclei with  $\gamma$ -H2AX associated signal presented rarely more than 1 focus, while in the double mutant the number of foci per nucleus could reach up to 12 (**Figure 2L**). Similarly, the diameter of the foci was rather constant in WT control nuclei, with an average around 0.2  $\mu\text{m}$ , while in *gip1gip2* it varied between 0.12 to more than 1.2  $\mu\text{m}$  with a mean diameter of 0.3  $\mu\text{m}$  (**Figure 2M**). Interestingly, among large foci ( $n = 81$ ; **Figures 2I,J**), 70% were detected at the nuclear periphery and 30% around the nucleolus. Smaller and less intense ones were distributed randomly through the nucleoplasm.

Consistent with the higher rate of DNA lesions measured by the comet assay, these results altogether indicate that *gip1gip2*



over-accumulates  $\gamma$ -H2AX foci that are heterogenous in size. These foci are notably found at the nuclear periphery close to the chromocenters.

## Differential Activation of the Double-Strand Break Repair Pathways in *gip1gip2*

Since we observed a constitutively high level of DSBs and numerous  $\gamma$ -H2AX foci in *gip1gip2*, we next investigated which DNA repair process was impaired. Firstly, we have checked the expression level of genes involved in the DSBs repair using quantitative real-time PCR (RT-qPCR). To this end, we selected genes encoding key factors involved in the two main DSB repair pathways: (i) the HR, restricted to cells in the S/G2 phase to resolve stalled replication fork and (ii) the non-homologous end-joining pathways (NHEJ) involved in repair of most DSBs (West et al., 2004). As representative of the HR pathway, we choose genes encoding HR regulators such as *BRCA1* (Lafarge and Montane, 2003) and *RAD9* (Heitzeberg et al., 2004), as well as the gene encoding the HR effector *RAD51* (Bleuyard et al., 2006). As indicative of the NHEJ pathway, *KU70* and *KU80* genes were analyzed for the classical NHEJ (c-NHEJ; Charbonnel et al., 2010), and the poly (ADP-ribose) polymerase encoding gene *PARP2* for the KU-independent backup-NHEJ (b-NHEJ) pathway (Jia et al., 2013). The expression of all tested genes was up-regulated in *gip1gip2*, indicating the activation of the DDR. However, contrary to those involved in NHEJ pathways, the genes representative of the HR pathway were the most induced in *gip1gip2* compared to WT (Figure 3). Indeed, *BRCA1* and *RAD9* encoding upstream regulators of HR, showed the highest fold change in their expression level, ranging between 6 and 9, respectively. The *RAD51* expression showed also a significant increase compared to WT with a 3.4-fold change, while the expression of NHEJ pathway genes (*KU70*, *KU80* and *PARP2*) remained only weakly induced (between 1.6- and 1.8-fold change).

In order to further determine which DNA repair pathway(s) were more specifically affected in *gip1gip2*, we next tested this double mutant in root growth assays in presence of the DNA damaging agents bleomycin (BLM) or cisplatin (CP). While the DSBs induced by BLM are classically repaired by both HR and NHEJ, the intra- and inter-strand DNA cross-links bridges induced by CP are preferentially repaired through HR during DNA replication (Fuertes et al., 2003). Therefore, we tested WT and *gip1gip2* root growth on media containing 10  $\mu$ M BLM and 50  $\mu$ M CP, respectively, as previously described (Roa et al., 2009; Biedermann et al., 2017). Contrary to WT plants in which root growth was similarly slowed down by BLM and CP, *gip1gip2* root growth appeared more affected upon CP treatment than upon BLM treatment (Figure 4 and Supplementary Figure 1). The higher sensitivity to CP (twice more compared to WT) than to BLM (decrease of only 1.2-fold) in *gip1gip2* is indicative of a predominant defect in HR repair.

Together, the major up-regulation of genes related to HR in *gip1gip2* and the increased sensitivity of the mutant to CP,

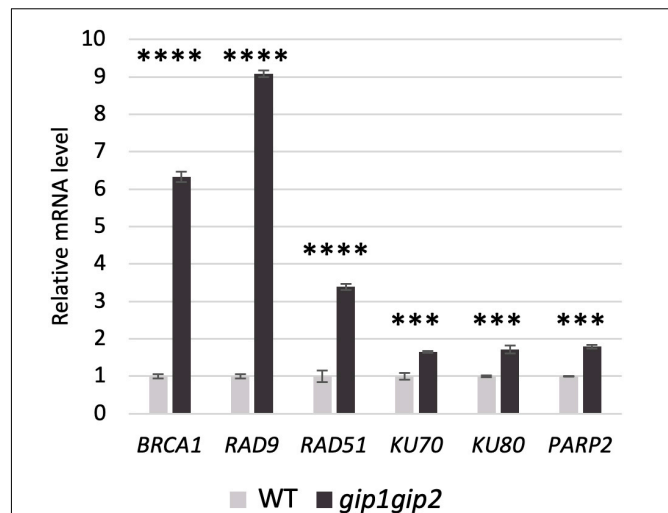


**FIGURE 3** | mRNA level of DNA damage responsive genes in *gip1gip2*. Relative mRNA level of selected DNA damage responsive genes in *gip1gip2* was compared to WT. Experiments of RT-qPCR was performed on RNA isolated from 9-day-old seedlings using specific set of primers (see Supplementary Table 1). Two independent experiments were performed. SDs are indicated. Unpaired *t* test was used where *p*-values are indicated as <0.0001 (\*\*\*\*) and <0.001 (\*\*\*), respectively.

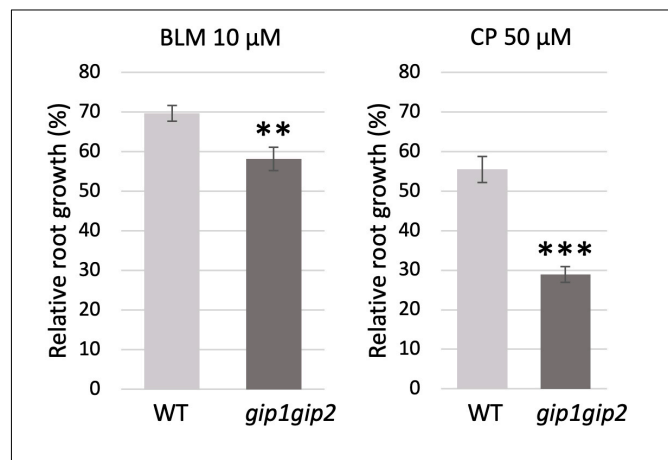


**FIGURE 4** | Sensitivity of *gip1gip2* toward drugs inducing DNA damage. Five-day-old seedlings grown on 1/2 MS media were transferred on 1/2 MS containing either 10  $\mu$ M bleomycin (BLM) or 50  $\mu$ M cisplatin (CP). Root growth was evaluated after 48 h on genotoxins in WT ( $n_{BLM} = 16$ ,  $n_{CP} = 19$ ) and *gip1gip2* ( $n_{BLM} = 20$ ,  $n_{CP} = 28$ ) (see Supplementary Figure 1). Percentages of relative root growth are presented. Two independent experiments were performed. SDs are indicated. The Fisher's exact test was performed and *p*-values are indicated as < 0.01 (\*\*) and < 0.001 (\*\*\*).

suggest that GIP1 and GIP2 may be important to regulate genome maintenance through HR in somatic cells.

## RAD51 and $\gamma$ -H2AX Foci Rarely Colocalized in *gip1gip2* Nuclei

In interphase nuclei from root meristems, the *gip1gip2* mutant accumulated a high number of  $\gamma$ -H2AX foci. This is indicative of defects in DNA repair, notably through HR, as shown by the

sensitivity of the mutant to CP. Thus, we further investigated the nuclear distribution of the HR effector RAD51. We performed co-immunolabeling on WT and *gip1gip2* root tip nuclei using together specific antibodies against RAD51 and  $\gamma$ -H2AX (Figure 5). As expected, a few nuclei showed RAD51 foci in WT (5.5%,  $n = 109$ ) which colocalized systematically with  $\gamma$ -H2AX foci (Figures 5A,B) as described previously (Biedermann et al., 2017). Such colocalization is further supported by fluorescence profiles presented in Figures 5A,B. In agreement with the increased number of  $\gamma$ -H2AX foci (Figure 2), the number of RAD51 foci was also significantly increased in *gip1gip2*, with 36% of nuclei showing RAD51 foci with an average of four per nucleus. Interestingly, the number of RAD51 foci per nucleus was significantly lower than the number of  $\gamma$ -H2AX foci and surprisingly most of the RAD51 foci showed no clear colocalization with  $\gamma$ -H2AX foci in *gip1gip2* (73%,  $n = 224$ ) (Figures 5C–E). In addition, 61% of the RAD51 foci were mainly found at/or very close to the bright DAPI-stained chromocenters (Figures 5C–E, see white arrows) without the

presence of  $\gamma$ -H2AX or no clear colocalization with  $\gamma$ -H2AX. Since a substantial decrease in the activity of GIP1 and GIP2 in the double knockdown mutant *gip1gip2* may impair RAD51 and  $\gamma$ -H2AX colocalization, we further explored the localization of GIP1-GFP upon genotoxic stress using CP. Using live cell imaging, GIP1-GFP in the nucleus appeared to be located close to the NE, as previously described (Janski et al., 2012; Batzenschlager et al., 2013; Batzenschlager et al., 2015) and this location was maintained when seedlings were treated by 50  $\mu$ M CP for 16 h (Figures 6A,B). As expected, compared to the control (Figure 6C), we observed that all RAD51 foci induced by CP colocalized with  $\gamma$ -H2AX foci using immunolabeling (Figure 6D, merge RAD51 and  $\gamma$ -H2AX), while 23% ( $n = 444$ ) of the RAD51 foci also colocalized with GIP1-GFP at the nuclear periphery (Figure 6D, merge RAD51 and GIP1-GFP with corresponding colocalization profiles).

Here, we showed that RAD51 and  $\gamma$ -H2AX foci are mostly not colocalizing in *gip1gip2* and that RAD51 foci are surprisingly located more frequently at chromocenters in

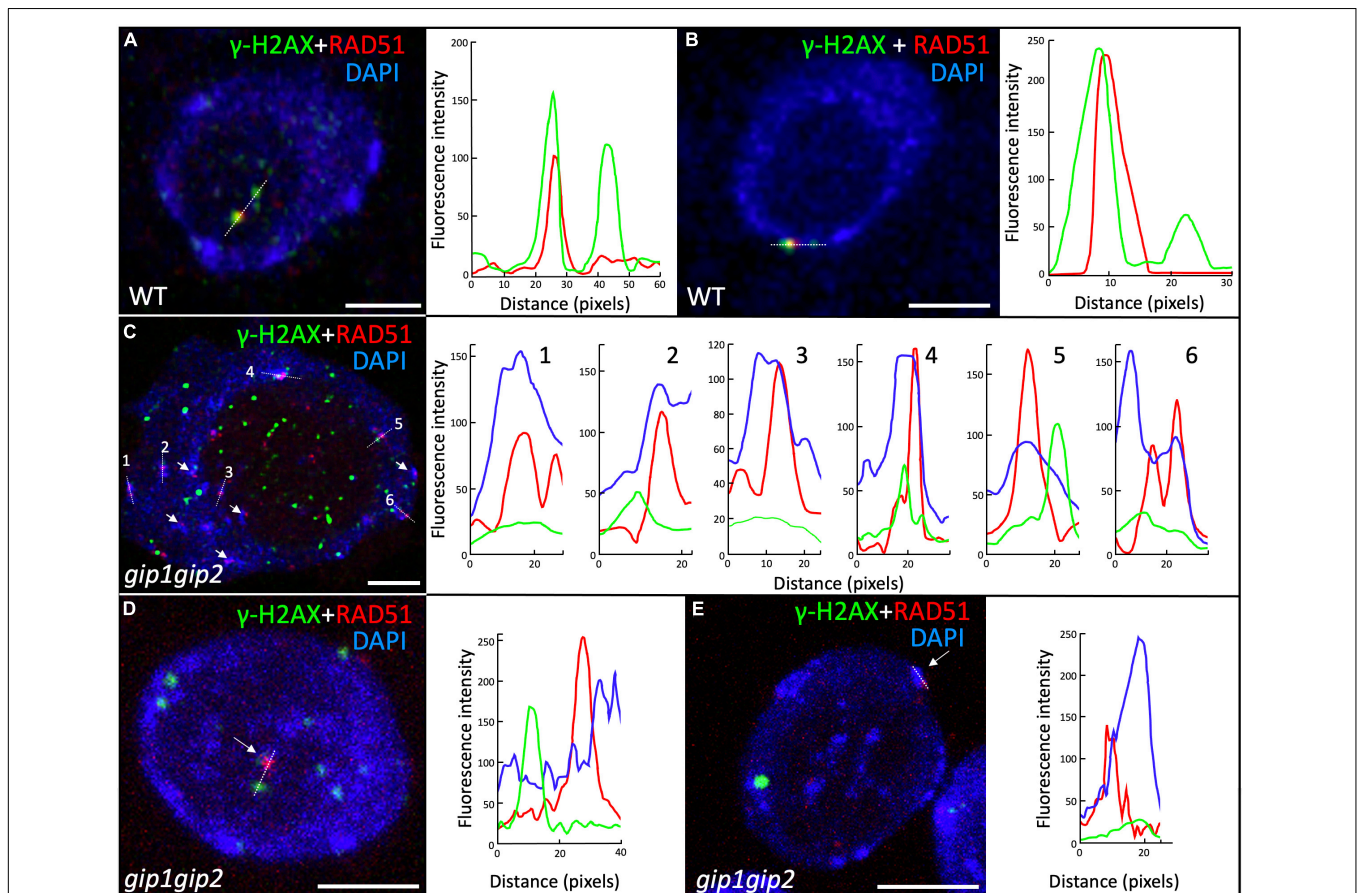


**FIGURE 5 |** Localization of the  $\gamma$ -H2AX and RAD51 foci in root meristematic nuclei. Immunolocalization was performed on 9-day-old seedlings root tip nuclei using antibodies against  $\gamma$ -H2AX and RAD51 together with a DAPI staining. Representative images of  $\gamma$ -H2AX and RAD51 foci in WT (A,B) and *gip1gip2* (C–E). Fluorescence profiles beside (A,B) illustrate the colocalization of  $\gamma$ -H2AX (green) and RAD51 (red) foci along the white dotted lines in WT. White arrows indicate RAD51 foci located at or close to bright DAPI-stained chromocenters in *gip1gip2*. Fluorescence profiles for  $\gamma$ -H2AX (green) and RAD51 (red) foci as well as high DAPI intensity for chromocenters (blue) are presented along the numbered white dotted lines indicated on the panels (C–E). This highlights that RAD51 foci are located at/or very close to chromocenters in *gip1gip2*. Scale bars = 5  $\mu$ m.

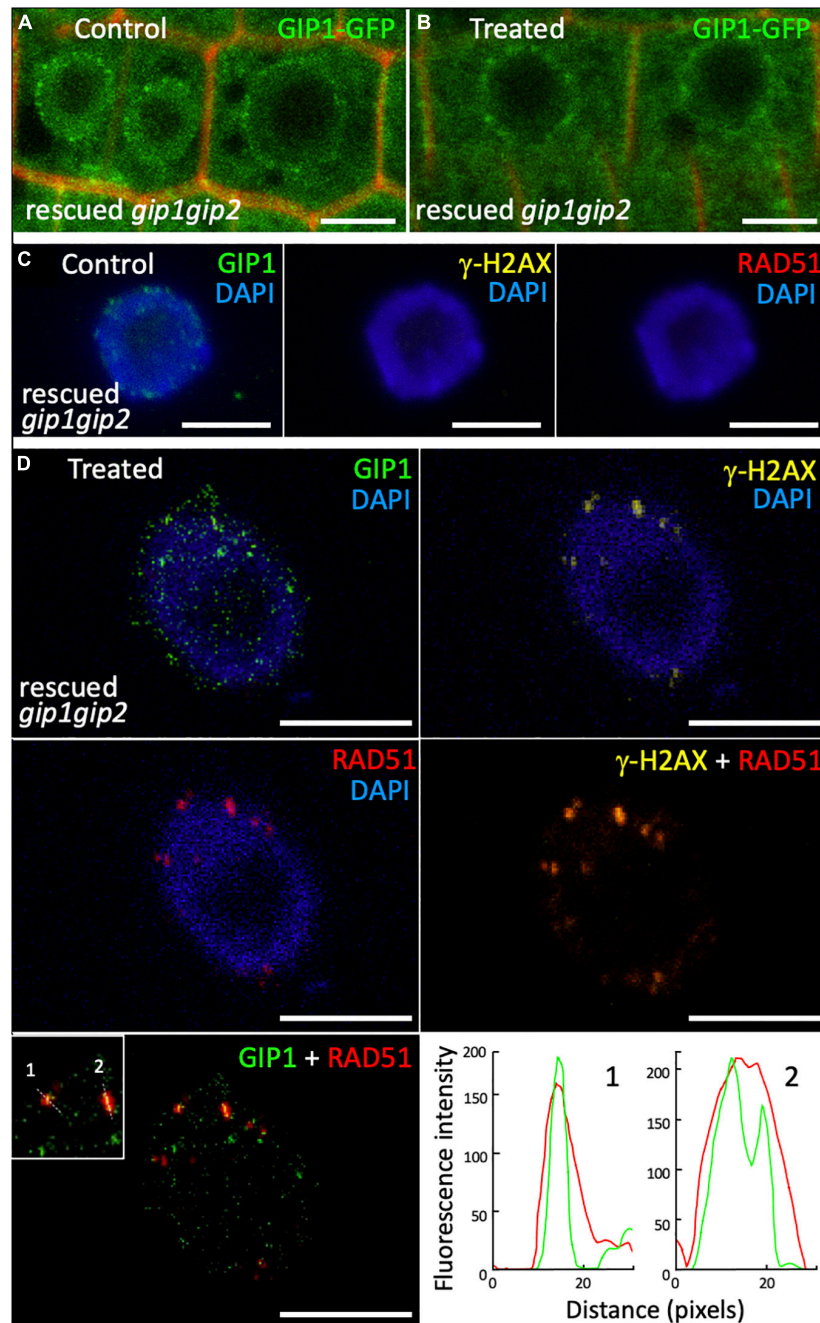


**FIGURE 6 |** Localization of GIP1-GFP in response to DNA damage induced by cisplatin. *GIP1-GFP* was expressed in the *gip1gip2* mutant and rescued cellular phenotypes as described (Batzenschlager et al., 2015). Nine-day-old seedlings were treated or not (control) by 50  $\mu$ M CP during 16 h in  $1/2$  MS. **(A,B)** GIP1-GFP localization was analyzed in root meristematic nuclei in control **(A)** and treated **(B)** cells. Cell wall was detected by propidium iodide staining. Representative images are presented. **(C,D)** Immunolocalization was performed on root tip nuclei using antibodies against GFP,  $\gamma$ -H2AX and RAD51 and DAPI staining. Two independent experiments were performed. Representative images of GIP1-GFP,  $\gamma$ -H2AX, and RAD51 foci are presented for control **(C)** and treated **(D)** cells. Merge images are presented for  $\gamma$ -H2AX (yellow) and RAD51 (red) as well as for GIP1-GFP (green) and RAD51 (red). Fluorescence profiles illustrate the colocalization of GIP1-GFP (green) and RAD51 (red) foci along the white dotted lines indicated on the left panel. Scale bars = 5  $\mu$ m.

the mutant. Interestingly in response to CP, RAD51, besides being systematically colocalized with  $\gamma$ -H2AX foci in the complemented mutant, partly colocalizes with GIP1-GFP at the nuclear periphery.

## DISCUSSION

In the present study we have investigated the genomic instability in the *gip1gip2* mutant which showed an increased DSBs

occurrence compared to the WT control. Besides the constitutive activation of the HR pathway, the mutant presented a stronger sensitivity to the genotoxic agent cisplatin, indicative of an impaired HR in root meristematic cells. This may rely on the absence of a clear expected colocalization between RAD51 and  $\gamma$ -H2AX foci in the mutant. Thus, we highlight novel functions of GIPs in the maintenance of genome stability at the nuclear periphery.

## How Genome Instability Occurs in *gip1gip2*

At the cellular level, numerous  $\gamma$ -H2AX foci are detected in *gip1gip2* and their heterogenous size may reach up to 2.5  $\mu$ m in diameter (Figure 2), indicating a permanent unrepaired DNA damage as described (Costes et al., 2006). This is contrasting with the low number of  $\gamma$ -H2AX foci which are smaller and more homogenous in size in WT, where active DNA repair occurs. As the mutant is mostly sensitive to cisplatin, this is indicative of a defective HR repair during DNA replication, leading to the accumulation of DSBs. Some of the  $\gamma$ -H2AX foci in *gip1gip2* are found at the nuclear periphery close to the chromocenters, which are mainly constituted by repetitive sequences and pericentromeric heterochromatin (Fransz et al., 2002). As centromeric heterochromatin organization was affected in *gip1gip2* (Batzenschlager et al., 2015), we cannot exclude defect in heterochromatin replication coupled with defective DNA repair. In this respect, we observed twice more late S-phase replicating nuclei in *gip1gip2* compared to WT (Supplementary Figure 2A), with the presence of  $\gamma$ -H2AX foci in the vicinity of late S-phase replicating DNA, mainly corresponding to pericentromeric heterochromatin (Supplementary Figure 2B). This defect in DNA repair could also explain the accumulation of G2-stalled 4C nuclei in *gip1gip2* (Janski et al., 2012; Batzenschlager et al., 2015). Alternatively, unscheduled RAD51 removal from DNA may also lead to its overaccumulation at stalled replication forks, as described in USO2 cells (Parplys et al., 2015). Thus, such overaccumulation leads to a decreased HR efficiency and an increased genomic instability. Together, besides the activation of the HR pathway, defects in DNA replication as well as abnormal RAD51 loading may result in the increased genomic instability observed in *gip1gip2*.

## Importance of the Nuclear Periphery for Genomic Maintenance in Plants

In plants,  $\gamma$ -H2AX form foci at DSB sites, where HR proteins such as RAD51 and RAD54 are sequentially recruited (Biedermann et al., 2017; Horvath et al., 2017; Meschichi et al., 2021). Moreover, RAD54 forms foci at DSBs that are restricted to S and G2 phase cells in roots (Hirakawa et al., 2017) and localized at the nuclear periphery close to the nuclear envelope at high frequency (Hirakawa and Matsunaga, 2019). Interestingly, this peripheral location was reduced in the double mutant for the plant nucleoskeleton components CRWN1 and CRWN4 after  $\gamma$ -irradiation (Hirakawa and Matsunaga, 2019). Furthermore, an interaction between RAD51 and RAD54 was already detected

in plants (Klutstein et al., 2008) and RAD54 may contribute to the removal of RAD51 at replication forks, as demonstrated in human cells (Mason et al., 2015). Together, we cannot exclude that, like for RAD51 which partially colocalized with GIP1 (Figure 6D), the function of RAD54 might also be affected in *gip1gip2* due to its possible impaired localization. Moreover, considering the crucial role of NPCs for DNA repair in animal and yeast (Freudenreich and Su, 2016), defects in the shape and the distribution of NPCs reported in *gip1gip2* (Batzenschlager et al., 2013) may also partially explain the defective HR repair we observed here. Together, GIP proteins may contribute to the spatio-temporal recruitment of RAD51 for efficient HR in genomic maintenance at the nuclear periphery.

## GIP at the Crossroad of DNA Repair and Cell Cycle Regulation

As GIPs are important to recruit microtubule (MT) nucleation complexes (Janski et al., 2012), we cannot exclude a role of either MTs or the  $\gamma$ -tubulin complex in the regulation of DNA repair. Indeed, MTs connected to the LINC complex were described to induce chromatin mobility around DSBs to promote efficient DNA repair in mammals (Lottersberger et al., 2015). Alternatively, an additional specific intranuclear function of GIPs and some of the MT nucleation complex proteins such as  $\gamma$ -tubulin, independent of MT dynamics and/or MT nucleation, may exist as well. Indeed, plant  $\gamma$ -tubulin was found at the inner membrane of NE in association with SUN1 (Chumova et al., 2019), and GIPs are also located on both sides of the NE (Batzenschlager et al., 2013; Batzenschlager et al., 2014).

GIPs are found at the nuclear periphery close to chromocenters (Batzenschlager et al., 2015). Interestingly, RAD51 localization at DNA lesions is mediated by RBR1 (Biedermann et al., 2017) which can form foci with  $\gamma$ -H2AX in the close vicinity of chromocenters (Horvath et al., 2017). In addition, both RAD51 and GIPs were shown to be substrates of the cell cycle regulators B1-type cyclin complexes (Motta et al., 2021), which activity drives the recruitment of RAD51 at DNA damage sites (Weimer et al., 2016). In line with this and similarly as our report on *gip1gip2*, *cycB1* mutants are mainly sensitive to cisplatin (Weimer et al., 2016). Altogether these data suggest that a dynamic crosstalk may involve GIPs as well as the cell cycle regulators RBR1 and B1-type cyclin complexes to allow proper loading of RAD51 at DNA lesions. However, the underlying mechanisms need to be further explored.

## CONCLUSION AND OUTLOOKS

Our data reveal an interesting role of GIPs at the nuclear periphery in the cross-talk between DNA replication and DNA repair in connection with chromatin organization. Indeed, our previous work had shown a synergism between GIPs and BRUSHY1 (BRU1)/MGOUN3 (MGO3)/TONSOKU (TSK) to maintain centromeric cohesion (Batzenschlager et al., 2017). BRU1 was also suggested to play a role in the structural and



functional maintenance of chromatin during DNA replication (Takeda et al., 2004; Suzuki et al., 2005). Nowadays, we need to further explore the role of both GIPs and BRU1 in the genomic maintenance at the nuclear periphery during DNA replication. Moreover, besides the abnormal shape of *gip1gip2* nuclei, we cannot exclude a rupture of the NE as a result of mechanically stressed nuclei (Goswami et al., 2020). Indeed, more rigid nuclei were described as defective in nuclear mechanics and thus triggering DNA damage in animals (Nava et al., 2020). This also opens the way to investigate the link between DNA repair and nuclear mechanics in plants.

## DATA AVAILABILITY STATEMENT

The original contributions presented in the study are included in the article/**Supplementary Material**, further inquiries can be directed to the corresponding author.

## AUTHOR CONTRIBUTIONS

M-EC: conceptualization, writing – original draft, and resources. M-EC and EHE: methodology. GS, MB, GH, EHO, DT, M-EC, and A-CS: investigation. AB, M-EC, GS, and MB: writing – review and editing. M-EC and AB: funding acquisition and supervision.

## REFERENCES

- Amiard, S., Gallego, M. E., and White, C. I. (2013). Signaling of double strand breaks and deprotected telomeres in *Arabidopsis*. *Front. Plant Sci.* 4:405. doi: 10.3389/fpls.2013.00405
- Batzenschlager, M., Herzog, E., Houlne, G., Schmit, A. C., and Chaboute, M. E. (2014). GIP/MZT1 proteins orchestrate nuclear shaping. *Front. Plant Sci.* 5:29. doi: 10.3389/fpls.2014.00029
- Batzenschlager, M., Lermontova, I., Schubert, V., Fuchs, J., Berr, A., Koini, M. A., et al. (2015). *Arabidopsis* MZT1 homologs GIP1 and GIP2 are essential for centromere architecture. *Proc. Natl. Acad. Sci. U S A.* 112, 8656–8660. doi: 10.1073/pnas.1506351112
- Batzenschlager, M., Masoud, K., Janski, N., Houlne, G., Herzog, E., Evrard, J. L., et al. (2013). The GIP gamma-tubulin complex-associated proteins are involved in nuclear architecture in *Arabidopsis thaliana*. *Front. Plant Sci.* 4:480. doi: 10.3389/fpls.2013.00480
- Batzenschlager, M., Schmit, A. C., Herzog, E., Fuchs, J., Schubert, V., Houlne, G., et al. (2017). MGO3 and GIP1 act synergistically for the maintenance of centromeric cohesion. *Nucleus* 8, 98–105. doi: 10.1080/19491034.2016.1276142
- Biedermann, S., Harashima, H., Chen, P., Heese, M., Bouyer, D., Sofroni, K., et al. (2017). The retinoblastoma homolog RBR1 mediates localization of the repair protein RAD51 to DNA lesions in *Arabidopsis*. *EMBO J.* 36, 1279–1297. doi: 10.15252/embj.201694571
- Bleuyard, J. Y., Gallego, M. E., and White, C. I. (2006). Recent advances in understanding of the DNA double-strand break repair machinery of plants. *DNA Repair (Amst)* 5, 1–12. doi: 10.1016/j.dnarep.2005.08.017
- Bukata, L., Parker, S. L., and D'Angelo, M. A. (2013). Nuclear pore complexes in the maintenance of genome integrity. *Curr. Opin. Cell Biol.* 25, 378–386. doi: 10.1016/j.ceb.2013.03.002
- Chaboute, M. E., and Berr, A. (2016). GIP contributions to the regulation of centromere at the interface between the nuclear envelope and the nucleoplasm. *Front. Plant Sci.* 7:118. doi: 10.3389/fpls.2016.00118
- Charbonnel, C., Gallego, M. E., and White, C. I. (2010). Xrcc1-dependent and Ku-dependent DNA double-strand break repair kinetics in *Arabidopsis* plants. *Plant J.* 64, 280–290. doi: 10.1111/j.1365-313X.2010.04331.x

GS, AB, and M-EC: figure preparation. All authors contributed to the article and approved the submitted version.

## FUNDING

This work was supported by the Centre National de la Recherche Scientifique (CNRS), by HFSP grant 2018, RGP, 009 and ANR REWIRE.

## ACKNOWLEDGMENTS

We thank J. Fuchs (IPK, Gatersleben) for providing us with flow sorted nuclei. We also thank S. Koechler, A. Alioua from the IBMP Gene Expression Analysis platform and J. Mutterer from the IBMP confocal microscopy platform for their technical help. We are grateful to P. Schlögelhofer for providing us the antibody against RAD51.

## SUPPLEMENTARY MATERIAL

The Supplementary Material for this article can be found online at: <https://www.frontiersin.org/articles/10.3389/fpls.2021.804928/full#supplementary-material>

- Cheng, Z., Zhang, X., Huang, P., Huang, G., Zhu, J., Chen, F., et al. (2020). Nup96 and HOS1 are mutually stabilized and gate constans protein level, conferring long-day photoperiodic flowering regulation in *Arabidopsis*. *Plant Cell* 32, 374–391. doi: 10.1105/tpc.19.00661
- Chumova, J., Kourova, H., Trogelova, L., Halada, P., and Binarova, P. (2019). Microtubular and nuclear functions of gamma-tubulin: are they LINCed? *Cells* 8:259. doi: 10.3390/cells8030259
- Collins, A. R. (2004). The comet assay for DNA damage and repair: principles, applications, and limitations. *Mol. Biotechnol.* 26, 249–261.
- Costes, S. V., Boissiere, A., Ravani, S., Romano, R., Parvin, B., and Barcellos-Hoff, M. H. (2006). Imaging features that discriminate between foci induced by high- and low-LET radiation in human fibroblasts. *Radiat. Res.* 165, 505–515. doi: 10.1667/RR3538.1
- Fenech, M., Kirsch-Volders, M., Natarajan, A. T., Surralles, J., Crott, J. W., Parry, J., et al. (2011). Molecular mechanisms of micronucleus, nucleoplasmic bridge and nuclear bud formation in mammalian and human cells. *Mutagenesis* 26, 125–132. doi: 10.1093/mutage/geq052
- Franz, P., De Jong, J. H., Lysak, M., Castiglione, M. R., and Schubert, I. (2002). Interphase chromosomes in *Arabidopsis* are organized as well defined chromocenters from which euchromatin loops emanate. *Proc. Natl. Acad. Sci. U S A.* 99, 14584–14589. doi: 10.1073/pnas.212325299
- Freudenreich, C. H., and Su, X. A. (2016). Relocalization of DNA lesions to the nuclear pore complex. *FEMS Yeast Res.* 16:fow095. doi: 10.1093/femsyr/fow095
- Friesner, J. D., Liu, B., Culligan, K., and Britt, A. B. (2005). Ionizing radiation-dependent gamma-H2AX focus formation requires ataxia telangiectasia mutated and ataxia telangiectasia mutated and Rad3-related. *Mol. Biol. Cell* 16, 2566–2576. doi: 10.1091/mbc.e04-10-0890
- Fuertes, M. A., Castilla, J., Alonso, C., and Perez, J. M. (2003). Cisplatin biochemical mechanism of action: from cytotoxicity to induction of cell death through interconnections between apoptotic and necrotic pathways. *Curr. Med. Chem.* 10, 257–266. doi: 10.2174/0929867033368484
- Gentric, N., Genschik, P., and Noir, S. (2021). Connections between the cell cycle and the DNA damage response in plants. *Int. J. Mol. Sci.* 22:9558. doi: 10.3390/ijms22179558

- Gentric, N., Masoud, K., Journot, R. P., Cognat, V., Chaboute, M. E., Noir, S., et al. (2020). The F-Box-Like protein FBL17 is a regulator of DNA-Damage response and colocalizes with retinoblastoma RELATED1 at DNA lesion sites. *Plant Physiol.* 183, 1295–1305. doi: 10.1104/pp.20.00188
- Goswami, R., Asnacios, A., Milani, P., Graindorge, S., Houlne, G., Mutterer, J., et al. (2020). Mechanical shielding in plant nuclei. *Curr. Biol.* 30, 2013–2025. doi: 10.1016/j.cub.2020.03.059
- Han, S. H., Park, Y. J., and Park, C. M. (2020). HOS1 activates DNA repair systems to enhance plant thermotolerance. *Nat. Plants* 6, 1439–1446. doi: 10.1038/s41477-020-00809-6
- Heitzberg, F., Chen, I. P., Hartung, F., Orel, N., Angelis, K. J., and Puchta, H. (2004). The Rad17 homologue of *Arabidopsis* is involved in the regulation of DNA damage repair and homologous recombination. *Plant J.* 38, 954–968. doi: 10.1111/j.1365-313X.2004.02097.x
- Hirakawa, T., and Matsunaga, S. (2019). Characterization of DNA repair foci in root cells of *Arabidopsis* in response to DNA damage. *Front. Plant Sci.* 10:990. doi: 10.3389/fpls.2019.00990
- Hirakawa, T., Hasegawa, J., White, C. I., and Matsunaga, S. (2017). RAD54 forms DNA repair foci in response to DNA damage in living plant cells. *Plant J.* 90, 372–382. doi: 10.1111/tpj.13499
- Horvath, B. M., Kourova, H., Nagy, S., Nemeth, E., Magyar, Z., Papdi, C., et al. (2017). *Arabidopsis* RETINOBLASTOMA RELATED directly regulates DNA damage responses through functions beyond cell cycle control. *EMBO J.* 36, 1261–1278. doi: 10.15252/embj.201694561
- Janski, N., Masoud, K., Batzenschlager, M., Herzog, E., Evrard, J. L., Houlne, G., et al. (2012). The GCP3-interacting proteins GIP1 and GIP2 are required for gamma-tubulin complex protein localization, spindle integrity, and chromosomal stability. *Plant Cell* 24, 1171–1187. doi: 10.1105/tpc.111.094904
- Jia, Q., den Dulk-Ras, A., Shen, H., Hooykaas, P. J., and de Pater, S. (2013). Poly(ADP-ribose)polymerases are involved in microhomology mediated back-up non-homologous end joining in *Arabidopsis thaliana*. *Plant Mol. Biol.* 82, 339–351. doi: 10.1007/s11103-013-0065-9
- Kerzendorfer, C., Vignard, C., Pedrosa-Harand, A., Siwiec, T., Akimcheva, S., Jolivet, S., et al. (2006). The *Arabidopsis thaliana* MND1 homologue plays a key role in meiotic homologous pairing, synapsis and recombination. *J. Cell Sci.* 119, 2486–2496. doi: 10.1242/jcs.02967
- Klutstein, M., Shaked, H., Sherman, A., Avivi-Ragolsky, N., Shema, E., Zenvirth, D., et al. (2008). Functional conservation of the yeast and *Arabidopsis* RAD54-like genes. *Genetics* 178, 2389–2397. doi: 10.1534/genetics.108.086777
- Lafarge, S., and Montane, M. H. (2003). Characterization of *Arabidopsis thaliana* ortholog of the human breast cancer susceptibility gene 1: AtBRCA1, strongly induced by gamma rays. *Nucleic Acids Res.* 31, 1148–1155. doi: 10.1093/nar/kgk202
- Lang, J., Smetana, O., Sanchez-Calderon, L., Lincker, F., Genestier, J., Schmit, A. C., et al. (2012). Plant gammaH2AX foci are required for proper DNA DSB repair responses and colocalize with E2F factors. *New Phytol.* 194, 353–363. doi: 10.1111/j.1469-8137.2012.04062.x
- Livak, K. J., and Schmittgen, T. D. (2001). Analysis of relative gene expression data using real-time quantitative PCR and the  $2^{-\Delta\Delta C(T)}$  Method. *Methods* 25, 402–408. doi: 10.1006/meth.2001.1262
- Lotterberger, F., Karssemeijer, R. A., Dimitrova, N., and de Lange, T. (2015). 53BP1 and the LINC complex promote microtubule-dependent DSB mobility and DNA repair. *Cell* 163, 880–893. doi: 10.1016/j.cell.2015.09.057
- Mason, J. M., Dusad, K., Wright, W. D., Grubb, J., Budke, B., Heyer, W. D., et al. (2015). RAD54 family translocases counter genotoxic effects of RAD51 in human tumor cells. *Nucleic Acids Res.* 43, 3180–3196. doi: 10.1093/nar/gkv175
- Meschichi, A., Reeck, S., Sicard, A., Pontvianne, F., and Rosa, S. (2021). Live-cell chromosome dynamics in *Arabidopsis thaliana* reveals increased chromatin mobility in response to DNA damage. *bioRxiv [preprint]* doi: 10.1101/2021.11.03.466744
- Motta, M. R., Zhao, X. A., Pastuglia, M., Belcram, K., Roodbarkelari, F., Komaki, M., et al. (2021). B1-type cyclins control microtubule organization during cell division in *Arabidopsis*. *EMBO Rep.* doi: 10.15252/embr.202153995 Online ahead of print.
- Nava, M. M., Miroshnikova, Y. A., Biggs, L. C., Whitefield, D. B., Metge, F., Boucas, J., et al. (2020). Heterochromatin-Driven nuclear softening protects the genome against mechanical stress-induced damage. *Cell* 181, 800–817. doi: 10.1016/j.cell.2020.03.052
- Noir, S., Marrocco, K., Masoud, K., Thomann, A., Gusti, A., Bitrian, M., et al. (2015). The control of *Arabidopsis thaliana* growth by cell proliferation and endoreplication requires the F-Box Protein FBL17. *Plant Cell* 27, 1461–1476. doi: 10.1105/tpc.114.135301
- Parplys, A. C., Seelbach, J. L., Becker, S., Behr, M., Wrona, A., Jend, C., et al. (2015). High levels of RAD51 perturb DNA replication elongation and cause unscheduled origin firing due to impaired CHK1 activation. *Cell Cycle* 14, 3190–3202. doi: 10.1080/15384101.2015.1055996
- Raynaud, C., and Nisa, M. (2020). A conserved role for gamma-tubulin as a regulator of E2F transcription factors. *J. Exp. Bot.* 71, 1199–1202. doi: 10.1093/jxb/erz557
- Roa, H., Lang, J., Culligan, K. M., Keller, M., Holec, S., Cognat, V., et al. (2009). Ribonucleotide reductase regulation in response to genotoxic stress in *Arabidopsis*. *Plant Physiol.* 151, 461–471. doi: 10.1104/pp.109.140053
- Roy, S. (2014). Maintenance of genome stability in plants: repairing DNA double strand breaks and chromatin structure stability. *Front. Plant Sci.* 5:487. doi: 10.3389/fpls.2014.00487
- Ryu, T., Spatola, B., Delabaere, L., Bowlin, K., Hopp, H., Kunitake, R., et al. (2015). Heterochromatic breaks move to the nuclear periphery to continue recombinational repair. *Nat. Cell Biol.* 17, 1401–1411. doi: 10.1038/ncb3258
- Suzuki, T., Nakajima, S., Inagaki, S., Hirano-Nakakita, M., Matsuoka, K., Demura, T., et al. (2005). TONSOKU is expressed in S phase of the cell cycle and its defect delays cell cycle progression in *Arabidopsis*. *Plant Cell Physiol.* 46, 736–742. doi: 10.1093/pcp/pci082
- Takatsuka, H., Shibata, A., and Umeda, M. (2021). Genome maintenance mechanisms at the chromatin level. *Int. J. Mol. Sci.* 22:10384. doi: 10.3390/ijms221910384
- Takeda, S., Tadele, Z., Hofmann, I., Probst, A. V., Angelis, K. J., Kaya, H., et al. (2004). BRU1, a novel link between responses to DNA damage and epigenetic gene silencing in *Arabidopsis*. *Genes Dev.* 18, 782–793. doi: 10.1101/gad.295404
- Varas, J., Graumann, K., Osman, K., Pradillo, M., Evans, D. E., Santos, J. L., et al. (2015). Absence of SUN1 and SUN2 proteins in *Arabidopsis thaliana* leads to a delay in meiotic progression and defects in synapsis and recombination. *Plant J.* 81, 329–346. doi: 10.1111/tpj.12730
- Wang, Q., Liu, S., Lu, C., La, Y., Dai, J., Ma, H., et al. (2019). Roles of CRWN-family proteins in protecting genomic DNA against oxidative damage. *J. Plant Physiol.* 233, 20–30. doi: 10.1016/j.jplph.2018.12.005
- Weimer, A. K., Biedermann, S., Harashima, H., Roodbarkelari, F., Takahashi, N., Foreman, J., et al. (2016). The plant-specific CDKB1-CYCB1 complex mediates homologous recombination repair in *Arabidopsis*. *EMBO J.* 35, 2068–2086. doi: 10.15252/embr.201593083
- West, C. E., Waterworth, W. M., Sunderland, P. A., and Bray, C. M. (2004). *Arabidopsis* DNA double-strand break repair pathways. *Biochem. Soc. Trans.* 32, 964–966. doi: 10.1042/BST0320964
- Ye, C. J., Sharpe, Z., Alemara, S., Mackenzie, S., Liu, G., Abdallah, B., et al. (2019). Micronuclei and genome chaos: changing the system inheritance. *Genes (Basel)* 10:366. doi: 10.3390/genes10050366

**Conflict of Interest:** The authors declare that the research was conducted in the absence of any commercial or financial relationships that could be construed as a potential conflict of interest.

**Publisher's Note:** All claims expressed in this article are solely those of the authors and do not necessarily represent those of their affiliated organizations, or those of the publisher, the editors and the reviewers. Any product that may be evaluated in this article, or claim that may be made by its manufacturer, is not guaranteed or endorsed by the publisher.

Copyright © 2022 Singh, Batzenschlager, Tomkova, Herzog, Hoffmann, Houlne, Schmit, Berr and Chaboute. This is an open-access article distributed under the terms of the Creative Commons Attribution License (CC BY). The use, distribution or reproduction in other forums is permitted, provided the original author(s) and the copyright owner(s) are credited and that the original publication in this journal is cited, in accordance with accepted academic practice. No use, distribution or reproduction is permitted which does not comply with these terms.